An investigation into the structure of poly(ethylene terephthalate) fibres by the use of optical transforms

G. Harburn and J. W. Lewis*
Physics Department, University College, PO Box 78, Cardiff CF1 1XL, UK

and J. O. Warwicker**
Shirley Institute, Didsbury, Manchester, M20 8RX, UK

An investigation has been made into the structural changes in poly(ethylene terephthalate) fibres brought about by drawing in a texturing machine. Evidence from both wide-angle and small-angle X-ray scattering is presented. The main feature of the small-angle X-ray scattering is a transition from two, meridional diffraction peaks to a symmetrical, four-point pattern as the draw ratio is increased. Optical transform methods have been used to investigate possible structural changes which could produce the observed transition. A tentative structure for poly(ethylene terephthalate) fibres is proposed.

(Keywords: poly(ethylene terephthalate); fibre structure; X-ray diffraction; optical transforms)

INTRODUCTION

The disposition of the main reflections in the small-angle X-ray scattering (SAXS) patterns of a number of polymers changes from a two-point to a four-point arrangement when the materials are processed in certain ways[1-3]. In the work of Warwicker[2] an investigation was made into the structural changes occurring in polyester during the simultaneous draw texturing process. The variables examined were applied draw ratio, temperature of heater, yarn speed and twist. The processing change that most-influenced the two-point to four-point transition was increase of draw ratio. Samples of similar yarns, but without twist applied, were supplied by the Shirley Institute and a further investigation has been made into the structural changes brought about by an increase in the applied draw ratio.

Peak positions and line-width analysis of wide-angle X-ray scattering (WAXS) and SAXS patterns do not yield an unambiguous statistical picture of the macrostructure because of the assumptions made in deriving structural parameters from the data. However, more information can be extracted from the SAXS patterns by the use of optical transform studies. In this technique a diffracting mask is made of any proposed stuctural model. The Fraunhofer diffraction pattern of this mask is produced in an optical diffractometer and the optical pattern compared with the SAXS pattern[4-6].

The crux of modelling in optical-transform studies is the identification of the essential parameters by which the proposed three-dimensional structure may be represented and the transformation of these parameters to give an equivalent two-dimensional arrangement. Thus the transparency distribution in the mask is an averaged projection of the scattering centres in a representative slice of material projected on to a plane containing the fibre axis. This representation of a three-dimensional structure in two dimensions is discussed further by Taylor[4] and Lewis[6].

The optical-transform method was used to study the scattering effects from a very wide range of possible models of polyester macrostructure. The models were based on inferences drawn from the WAXS and SAXS patterns and on current visualizations of macrostructure contained in the literature. The design of the models was also influenced by evidence from investigations using other techniques, such as infra-red absorption and electron microscopy.

Many current models are based on fibrillar elements with a two-phase system of crystalline and amorphous regions, of high and low electron densities respectively. These features were the starting point for the studies. The models developed to include fibrils with high and low-electron density regions along their length, in which regions were either rectangular or parallelogram-shaped in projection. Later, rectangular crystallites, both with and without crystalline links were investigated and, finally, the effects of loss of fibrousness were studied.

In all, about 200 masks were prepared and their diffraction patterns studied. Consideration of all the evidence leads to a tentative proposal for the macrostructure of drawn poly(ethylene terephthalate).

EXPERIMENTAL

Materials

All the samples were processed and supplied by The Shirley Institute. The control yarn, sample V2C, was an experimental, partially-oriented yarn of Viscosuisse with an initial decitex of 268 and a residual draw ratio of 1.62. Samples S1 to S5 were yarns that had been drawn at 200 m/min over the heater, which was at 220°C, of a

texturing machine but with no twist applied. The applied draw ratios (ADR) for these samples were 1.51, 1.57, 1.62, 1.65 and 1.72 respectively. Two thermally annealed yarns were also supplied; V2T, which was annealed under tension at constant length in an oven at 220°C, and V2NT, a similar sample which was left to contract freely during annealing at 220°C.

X-ray and microdensitometer measurements

A modified Warhus camera was used to record both WAXS and SAXS patterns. The collimator consisted of two, 0.3 mm diameter pinholes 305 mm apart. Samples were prepared from 10 mg of the fibre which was wound on a former with just sufficient tension to keep the individual strands parallel. Each bundle was carefully bound at its ends to retain this parallelism before being removed from the former and mounted in the X-ray camera immediately after the second pinhole. Thus, for each sample, there was the same weight of material in the X-ray beam though the linear density of the fibre varied from sample to sample. The WAXS and SAXS patterns were recorded on flat sheets of Ilford Industrial G film at distances from the sample of 68 mm and 312 mm respectively. The X-ray generator was operated at 36 kV and 24 mA. Nickel-filtered $CuK\alpha$ radiation was used and exposures varied from 1 to 4 days. The camera was evacuated during exposures, the durations of which were chosen so that the optical densities of the processed films were within the range which bore a linear relation to the X-ray exposure.

Microdensitometer scans of the WAXS patterns were made both along the equator and along a line at about 40° to the equator. The latter direction was chosen because it passes through a region which does not contain any discrete reflections. This isotropic, background scatter was subtracted from the equatorial scans and the residual scatter analysed. The line-widths measured for the equatorial reflections involved three broadening factors. First, broadening due to the size of crystalline regions in the sample (the required quantity), secondly, instrumental broadening due to the finite diameter of the X-ray beam and, thirdly, microdensitometer broadening due to the finite size of the scanning aperture. For WAXS the two latter effects were shown to be negligible so that the difference between the two microdensitometer scans could be taken directly as a measurement of sample line width. In addition, azimuthal scans were taken for the 100 reflections to determine values for $\phi_{1/2}$, the angular half-width at half the maximum intensity. This parameter[7] is discussed later.

For each SAXS photograph, microdensitometer scans were made both along the meridian and along the layer lines. The former was used only to locate the position of maximum scattered intensity from which the long-period spacing was obtained. The layer-line scans were used to estimate the lateral extent of crystallites and were corrected for instrumental broadening. Microdenistometer broadening was negligible and was ignored.

Optical transforms

Optical diffraction masks representing proposed macrostructures were prepared on photographic film using an Optronics P1500 Photowrite system. In this equipment an illuminated aperture is imaged on to the film which is exposed sequentially, in raster fashion, at the

points of a square lattice. At the highest resolution the lattice spacing is 25 μm so that up to 8×10^7 data points can be included on the full 250 mm $\times$ 200 mm sheet of film. Two other lattice spacings, of 50 μm and 100 μm are available. The dimensions of the illuminated aperture are chosen to match the lattice spacing so that the square dots, printed at adjacent lattice points, just touch. In practice, for the majority of masks, the information about the proposed structure was contained within a circle of about 100 mm diameter. Each dot on the film can be printed at any chosen grey level on a scale 0 to 255. The optical density associated with level 255 depends on the processing conditions but, for masks containing only clear and opaque regions corresponding to a two-phase structural model, would normally be about 2.0. The data defining the grey level required at each lattice point is generated in a computer and output on to magnetic tape, which then forms the input to the Photowrite tape reader[6,8]. The Fraunhofer diffraction patterns of these masks were produced in a high-quality optical diffracto-meter using a helium–neon laser as the coherent light source[9]. The diffraction patterns were photographed at several different exposures so that the most-suitable intensity level was available for comparison with the SAXS patterns.

RESULTS

Wide-angle X-ray scattering

Two of the WAXS patterns are shown in *Figure 1*. The sharp ring present in all the patterns is due to the small percentage ($\simeq 0.5\%$) of titanium dioxide delustrant present in the commercial polyester.

For the control sample V2C there is no sign of crystallinity but some evidence of orientation in that the diffuse ring has an intensity maximum on the equator. The patterns for samples S1 to S5 and V2T show that these are partially crystalline with reasonable axial orientation. That for V2NT shows that this sample is poorly oriented.

It was assumed that the material of the samples was closely similar to that for which detailed crystallographic studies have been made by, for example, Daubeny, Bunn and Brown[10] and Arnott and Wonacott[11]. The main reflections of the WAXS patterns could therefore be indexed by inspection with reference to the established structural work. It should be noted that the long, c-axis of the triclinic unit cell does not necessarily coincide exactly with the fibre axis[10]. Crystal lattice spacings were found from the Bragg equation using the 100 and 010 reflections. Values of $a = 3.45$ Å and $b = 5.05$ Å were obtained, to
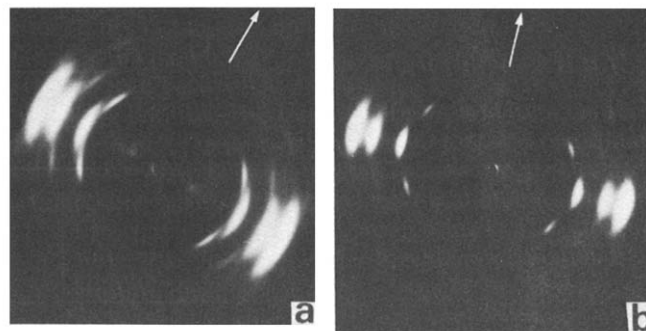

Figure 1 Wide-angle X-ray scattering patterns for (a) sample S1, (b) sample S3. The arrows show the direction of the fibre axis
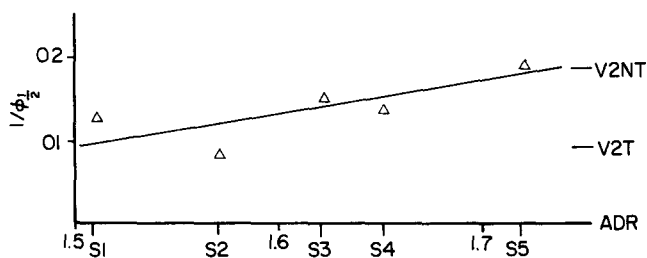
Figure 2 Variation of orientation parameter $1/\phi_{1/2}$ with draw ratio

within $\pm 2\%$, for all samples except V2NT which could not be analysed because the poor orientation meant that reflections other than the 100, 010 and 110 were contributing significantly to the equatorial intensity distribution.

The minimum crystallite dimensions in the a and b directions, D_{100} and D_{010}, were determined from the broadening of the 100 and 010 reflections using the Scherrer equation[12]. These parameters must be used with some caution but, for samples S1 to S5, D_{100} and D_{010} remained constant (to within about 10%) at 28 Å and 45 Å respectively. The V2T sample showed significantly higher values with $D_{100} = 34$ Å and $D_{010} = 53$ Å; values could not be obtained for V2NT.

The WAXS pattern of polyester fibre contains no suitable meridional reflection for assessment of molecular orientation. Although the $\overline{1}05$ reflexion has been used by some workers[13] there are difficulties in resolving the $\overline{1}05$ and 024 reflexions. However, Warwicker[14] and others have agreed that, provided reasonable axial orientation has been achieved, the orientation of the (100) planes can be used to describe molecular orientation. *Figure 2* shows the increase of the orientation parameter, $1/\phi_{1/2}$, with applied draw ratio. The appearance of the WAXS patterns for different values of draw ratio depends on the starting material used. Liska[3], for example, has shown patterns which clearly demonstrate that the orientation in PET fibres is biaxial. In some cases the 100 reflection occurs initially on the meridian whereas in others it occurs on the equator as found in the present studies.

The parameter $X = I_c\phi_{1/2}/I_a$, where I_c is the equatorial peak height, after subtraction of the background, of the 100 reflection and I_a is the peak height of the amorphous halo, gives a crude measure of the volume ratio of crystalline and amorphous material in each sample according to Miller[15]. This crystallinity index remained constant, within the limits of experimental error, over the range of draw ratio investigated.

Small-angle X-ray scattering

Figure 3 shows a typical SAXS pattern. With the exception of V2C, all the samples give patterns with layer lines, which tend to become four-pointed as the draw ratio increases. A short equatorial streak is present in all patterns except that for V2NT but including V2C. Comparison of the isotropic scattering around the back-stop both with and without samples in the beam lead to the conclusion that this scattering was due to the camera and that there was no isotropic contribution from the samples at angles corresponding to periodicities between 150 Å and 220 Å, the limit of resolution for the camera.

The meridional microdensitometer scans were used to calculate the long periods which are shown in *Figure 4*. Microdensitometer scans along the layer lines, i.e. at right

angles to the fibre axis, showed clearly the tendency to a four-point arrangement which is evident in *Figure 3(c)* for samples with higher draw ratios. The angular half-height widths of the layer line scans were measured and corrected for instrumental broadening to give the parameter $\delta\phi$. If it is assumed that the width of the reflection is due solely to crystallite size (Kukesenko[16]) then a measure of the lateral extent of the crystallite is given by $D_{\delta\phi} = \lambda/\delta\phi$ where λ is the wavelength of the X-rays. For S1, S5 and V2T the values of $D_{\delta\phi}$ were 65 Å, 23 Å and 50 Å, respectively. Kukesenko's assumption may be a good approximation for samples of low draw ratio, which give a two-point pattern, but for SAXS which has quadrantal tendencies the lateral dimension will be underestimated. With this point in mind the values of $D_{\delta\phi}$ correlate well with the minimum crystallite size deduced from the WAXS.

Optical transforms

The more important models that were studied are summarized in *Table 1*, which also includes comments on their diffraction patterns and the ways in which these patterns change as the various parameters are altered. Most of the parameters were variables and the ranges of values that were used are given. For any individual model by no means all of the possible combinations of the parameter values quoted have been investigated, either because a combination was not physically realisable or because its optical pattern would not have been sufficiently different from others in the sequence to merit examination. Linear dimensions are in Photowrite units (pwu) one of which corresponds to one Photowrite lattice translation. To give a reasonable statistical representation most of the parameters, e.g. W, within a given mask were allowed to vary according to a Gaussian distribution of standard deviation, e.g. $\sigma(W)$. Where other distribution
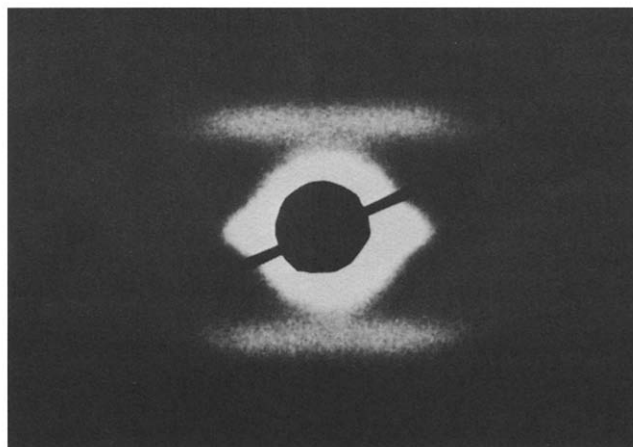

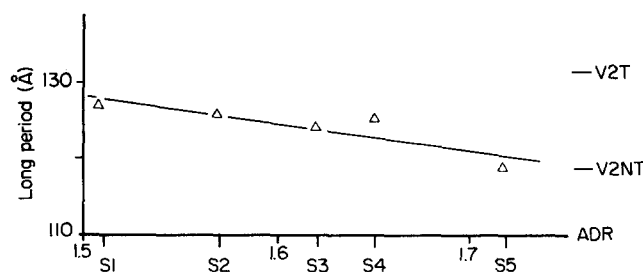**Figure 3** Small-angle X-ray scattering pattern for sample S5

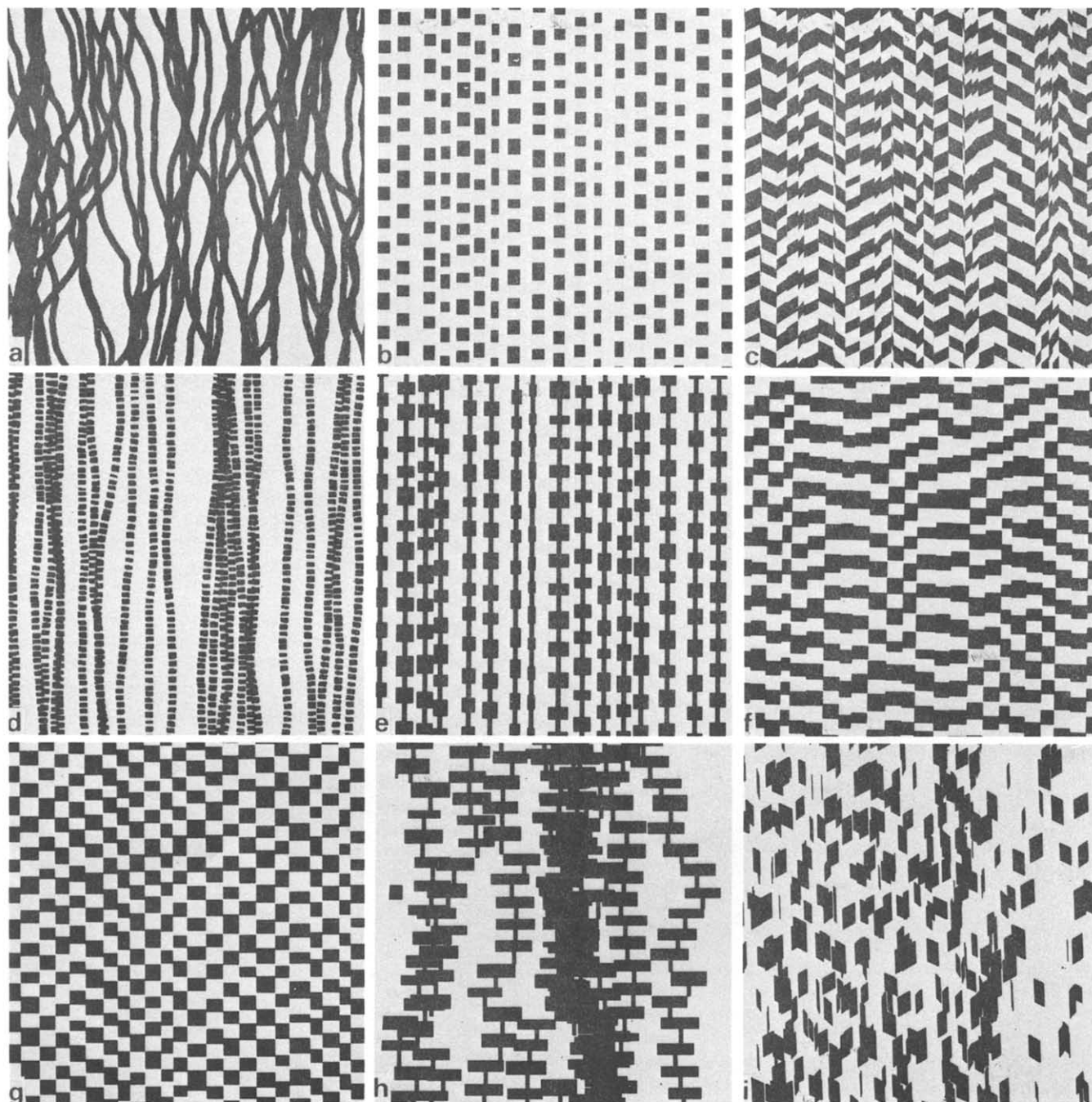**Figure 4** Variation of long period with draw ratio

Figure 5 Examples of masks according to the following models (see *Table 1*). (a) 1.3, (b) 2.1, (c) 2.3, (d) 2.4, (e) 2.5, (f) 3, no correlation, (g) 3, with correlation, (h) 4.1, (i) 4.2

functions were used their form is stated. In the fibrillar models the width W is constant for any one fibril but can vary from fibril to fibril.

Table 1 contains all the essential information but, as an aid to visualization, sample regions of some masks representing different models, not all to the same scale, are shown in *Figure 5*. In the Figure, black and white regions correspond to crystalline and amorphous phases respectively. In an actual mask, diffraction contrast was obtained by representing crystalline and amorphous phases by clear and opaque regions respectively.
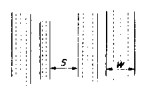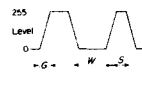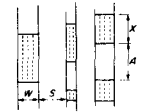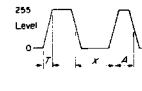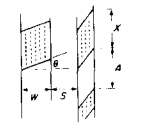
Two of the models require further comment here.

(a) Imperfectly oriented fibrils. The factors which affect the angle between the fibre axis and any short length of a fibril are many and undoubtedly complicated but they

have been reduced to two for the purposes of modelling. First, a parameter O which limits the overall orientation of a fibril segment with respect to the fibre axis; this parameter will be closely related to the drawing process. Secondly, a fibril flexibility parameter F, which controls the angle between adjacent segments of the fibril. Taken together these parameters give a distribution, of half width $\delta\psi$, for the angles between fibril segments and the fibre axis. A particular value of $\delta\psi$ can be achieved by different combinations of the orientation and flexibility parameters but is, nevertheless, a useful measure of misorientation.
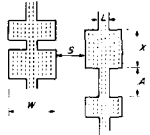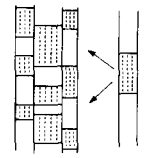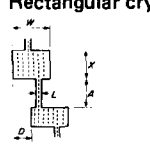
(b) Laterally correlated fibrils. When the space between the fibrils is small or absent, the way in which adjacent fibrils will pack together must be considered. A packing

Table 1 Models investigated, the parameters used to describe them and comments on their diffraction patterns. Two-phase models have amorphous regions printed white, crystalline regions are hatched. Linear dimensions are in Photowrite units. The range chosen for each parameter is shown together with, in brackets, the number of values from that range that was actually used

Model		Parameter values		Comments on main features and trends in optical transforms
1.	**CRYSTALLINE FIBRILS**			
1.1	Sharp edges	W	10–30, (3)	Increase in W reduces the spacing of the equatorial maxima
		σ (W)	0–40, (7)	
		S	Taken from uniform distribution between 1 and 50	Increase in σ (W) causes the peak intensity to be smeared out along the equator
1.2	Gradual transition in density at fibril edges	W	10–30, (3)	Higher values of G give sharper equatorial peaks even for values of $\sigma(W)/W$ as high as 0.5.
		$\sigma(W)$	0–40, (7)	
		S	Taken from uniform distribution between 1 and 50	
		G	3,9.	
1.3	Imperfectly oriented fibrils Misorientation in the plane of the mask controlled by parameters O and F (see text) which lead to an angular distribution of fibril segments of half-width $\delta \psi$	W	10	Equatorial streak fans out as $\delta \psi$ increases. For a given $\delta \psi$ the amount of fanning depends on precise values of O and F, but their independent significance appears to be secondary. Within wide limits the amount of overlap and the packing density of the fibrils have little effect on the pattern.
		σ (W)	0	
		S	Not applicable, See *Figure 5(a)*	
		$\delta \psi$	0°–75°, (11)	
2.	**TWO-PHASE FIBRILS**			
2.1	Rectangular crystallities	W	5–80, (4)	Low values of $\sigma(X)$ and/or σ (A) give highly detailed patterns with many sharp layer lines of spacing corresponding to a long period ($X + A$). Zero layer line is a series of sharp spots of spacing corresponding to ($W + S$). As σ (W) and/or σ (S) increase, layer lines smear out equatorially and equatorial spots smear out to give a streak. As σ (X) increases, layer lines become diffuse and eventually disappear leaving just a diffuse first layer-line. The result is similar if both σ (X) and σ (A) are increased, but is achieved for lower values. At medium values of σ (X) the layer line spacings are not constant, giving rise to ambiguity in the long period deduced from the pattern. Change in the ratio X/A can enhance the intensity of the second layer line while higher orders remain weak and diffuse. As W and/or S increases, the equatorial peaks move to lower angles
		σ (W)	0–30, (4)	
		S	0–30, (4)	
		σ (S)	0–30, (4)	
		X	5–30, (4)	
		σ (X)	0–30, (5)	
		A	30–55, (4)	
		σ (A)	0–20, (4)	
2.2	Density transition along the fibril As for 2.1 but with a linear change in grey level between crystalline and amorphous blocks	X	5–30, (4)	Meridional broadening of layer lines is much less than when $T = 0$ but higher layers are more rapidly suppressed (or first layer enhanced) for all values of σ (X) and σ (A). As X/A departs from 1, layer lines stay sharp but higher orders remain strong
		σ (X)	0–30, (5)	
		A	30–55, (4)	
		σ (A)	0–30, (4)	
		W	5–80, (4)	
		σ (W)	0–30, (4)	
		S	0	
		σ (S)	0	
		T	12	
2.3	Parallelogram-shaped crystallities As 2.1 but crystalline and amorphous regions in fibrils have parallelogram shape	X	5–30, (5)	A general feature is an X shape, symmetrical about the meridian (and equator) which modifies features produced by earlier models. Sharp cut-off on meridian above first layer line when σ (X) and σ (A) > 5. First layer line shows tendency to split giving a four-point pattern which is pronounced for high values of W. Values of X/σ (X) and $A/\sigma(A)$ between 5 and 3 give a good two point pattern. Patterns relatively insensitive to the values of σ (W)
		σ (X)	0–30, (5)	
		A	30–55, (5)	
		σ (A)	0–30, (5)	
		W	30–120. (6)	
		σ (W)	5–50, (4)	
		S	10–50, (3)	
		σ (S)	5–30, (4)	
		θ	25°–65° (5)	
	Model designed to represent crystalline faceting and based on tape-like fibrils. Basic value for θ applies to tape which is parallel to the projection plane. When fibril rotates the projected value of θ increases while W decreases. Individual fibrils are rotated by a fixed amount, i.e. the tapes do not twist along their lengths			

Table 1 *continued*

Model	Parameter values		Comments on main features and trends in optical transforms
2.4 Rectangular crystallites with misorientation of fibrils A combination of models 1.3 and 2.1	X $\sigma(X)$ A $\sigma(A)$ W $\sigma(W)$ S $\delta\,\psi$	30 6, 15 30 6, 15 10 0 Not applicable. See *Figure 5* 5°, 70°	Two-point patterns with diffuse layer lines when $\delta\,\psi$ small. Layer lines absent when $\delta\,\psi$ large
2.5 Rectangular crystallites with crystalline links W is constant for any one fibril the links for which are co-linear L is constant in any one mask 	X $\sigma(X)$ A $\sigma(A)$ W $\sigma(W)$ $S.$ $L.$	30 5 30 5 30 5 Taken from uniform distribution between 0 and 30. 1–15, (4)	As L increases, an initially spotty equatorial streak contracts to give two spots astride the origin while the first layer line sharpens meridionally, extends equatorially and splits to give three, highly-elongated spots
3. LATERALLY CORRELATED FIBRILS For explanation, see text.	X $\sigma(X)$ A $\sigma(A)$ W $\sigma(W)$ Correlation routine is either in use or suppressed	10–50, (5) 0–30, (5) 10–50, (5) 0–30, (5) 15–85, (4) 0–30, (5)	Generally, correlation changes the pattern dramatically from two- to four-point. The positions of the four points are governed by the ratio $(X+A)/W$ the points being closer to the meridian for high values of W Higher layers are prominent when X/A is large and $\sigma(X)$ or $\sigma(A)$ small. As $\sigma(X)$ and/or $\sigma(A)$ increased, higher layers disappear, the four points become diffuse, both equatorially and meridionally and tend to merge. However, for high $\sigma(X)$ the first layer line is convex as seen from the origin whereas for high $\sigma(A)$ it is concave. As $\sigma(W)$ increased, first layer lines become two points but remain narrow in the meridional direction
4. LOSS OF FIBROUSNESS A displacement parameter is introduced into 2.5 so that crystallites are not restricted to a fibre axis			
4.1 Rectangular crystallites If $D \neq 0$, a preferential fibril growth direction is introduced. Links are parallel to the fibre axis. They are randomly positioned along the crystallite edges within the lateral overlap region for adjacent crystallites along the fibril length	X $\sigma(X)$ A $\sigma(A)$ W $\sigma(W)$ D $\sigma(D)$ L	30 5 30 5 30 5, 10, 20 0, ± 101± 20, ± 30 0–20, (4) 0, 5.	With $L = 0$ $D = 0$, increase in $\sigma(W)$ gives decrease in layer line intensity and increase in general background. Increase in $\sigma(D)$ causes layer lines to fan out at ends. If $D = 0$, layer lines are tilted. When $L = 0$ equatorial scatter is enhanced. Comparison with 2.5 suggests that the positions of the links have little effect on the patterns

continued ...

Table 1 *continued*

Model		Parameter values		Comments on main features and trends in optical transforms
4.2	Parallelogram-shaped crystallites	X	30	As $\sigma(D)$ increased the layer lines fan out until they meet, giving sharp but weak meridional reflections with extended diffuse regions elsewhere. Scant resemblance to any SAXS patterns
		$\sigma(X)$	5	
		A	30	
	As 4.1, but with the crystallites of 2.3	$\sigma(A)$	5	
		W	30	
		$\sigma(W)$	5	
		D	0	
		$\sigma(D)$	0–50, (4)	
		L	0	
		θ	25°	

scheme similar to that envisaged by Statton[17] was adopted. Fibrils are considered to be made up of bulky amorphous and compact crystalline segments forming a structure rather like a string of beads. One fibril was laid down and subsequent ones grown alongside, in turn, subject to constraints which adjusted the parameters chosen from the basic distributions to improve the lateral correlation between crystalline and amorphous regions.

It is impractical to show sequences of optical transforms for all the models but one series is presented in *Figure 6* as an indication of the appearance of the diffraction patterns and to show the sorts of changes that can occur as the parameters for one particular model are altered. The parameters for the masks used for *Figure 6* are shown in *Table 2*. For a full presentation of the masks and transforms and for a more detailed discussion of their interpretation than is given in *Table 1*, the reader is referred to Lewis[6].

DISCUSSION

It has been observed (*Figure 3*) that when the draw ratio is increased the SAXS changes from a two-point to a four-point pattern. At the same time the WAXS patterns show an increase in axial orientation. Thus the two- to four-point transition arises in material which is becoming well-aligned axially.

The optical diffraction experiments show that the transition from a two- to a four-point diagram can be achieved in a number of ways and it is desirable to decide which model is the most consistent with the evidence available. There is, however, one clear conclusion that can be made immediately, namely that it is not necessary to assume regular folded chains to explain the SAXS evidence. Such evidence can be explained by changes in the shape and disposition of the diffracting units and is not directly concerned with their internal structure.

To obtain a two-point pattern, a lattice with at least some one-dimensional order along the fibre axis must be present but a small degree of misorientation of the crystallites is permissible. However, it is not necessary to invoke uniform fibrillar structure and imperfect fibrillar register of the crystallites is allowable to some extent. To achieve a pattern containing only one order of diffraction, as in SAXS patterns, requires that either the lattice order along the fibre axis must be very poor, leading to a diffuseness not found in all two-point patterns, or the crystalline and amorphous segments along the fibre axis must be of the same order of size, when a gradual transition of electron density between them also helps to

suppress the high orders. If two-phase fibrillar elements are present they must be tightly packed otherwise a strong equatorial streak is formed and such is not found in the SAXS patterns. Similarly, crystalline links joining crystallites in the fibre direction cannot be present in any significant number since they also give rise to appreciable equatorial scattering. This consideration therefore rules out any appreciable amount of shish-kebab types of structure in drawn polyester fibres. By the Babinet theorem, equatorial scattering could be due to voids elongated in the fibre direction but, if they do exist, their volume must be very small because they would scatter strongly since they have high electron-density contrast with their surroundings.

The change in meridional position of the SAXS peaks that was observed in these experiments can be explained in terms of changes in either the shape of the scattering unit or the order along the fibril. However, the simultaneous requirement of a two to four-point transition limits the types of structure that are possible. The optical diffraction studies showed that the two- to four-point transition can be due to the angle of crystalline facets, and changes to this angle, combined with a suitable value of the ratio of the fibril repeat length to repeat width. Plausible lattice-order mechanisms for the transition were confined to models which depended on the introduction of a measure of two-dimensional order in a basically one-dimensional model, i.e. on packing correlation. Within this broad category the following parameters were important. Mean fibril width and standard deviation, ratio of mean lengths of crystalline and amorphous segments and the two standard deviations in the size distributions of these segments. Preferential stagger alone cannot be responsible for the two- to four-point transition.

From a purely geometric standpoint these mechanisms, deduced from the optical transform studies, give possible explanations for the two- to four-point transition observed in the SAXS. It is possible that in different polymers the mechanism for this transition will be different so that it is necessary to find the mechanism consistent with the data obtained for polyester as given here.

It must be kept in mind that for the original partially-oriented yarn neither the WAXS nor the SAXS gives evidence of either crystalline or long-range order, although the WAXS does suggest some slight molecular orientation along the fibre axis. The molecular chains must therefore be largely randomly dispersed in the fibre and are probably randomly coiled or kinked with a slight tendency to orientate along the fibre axis.

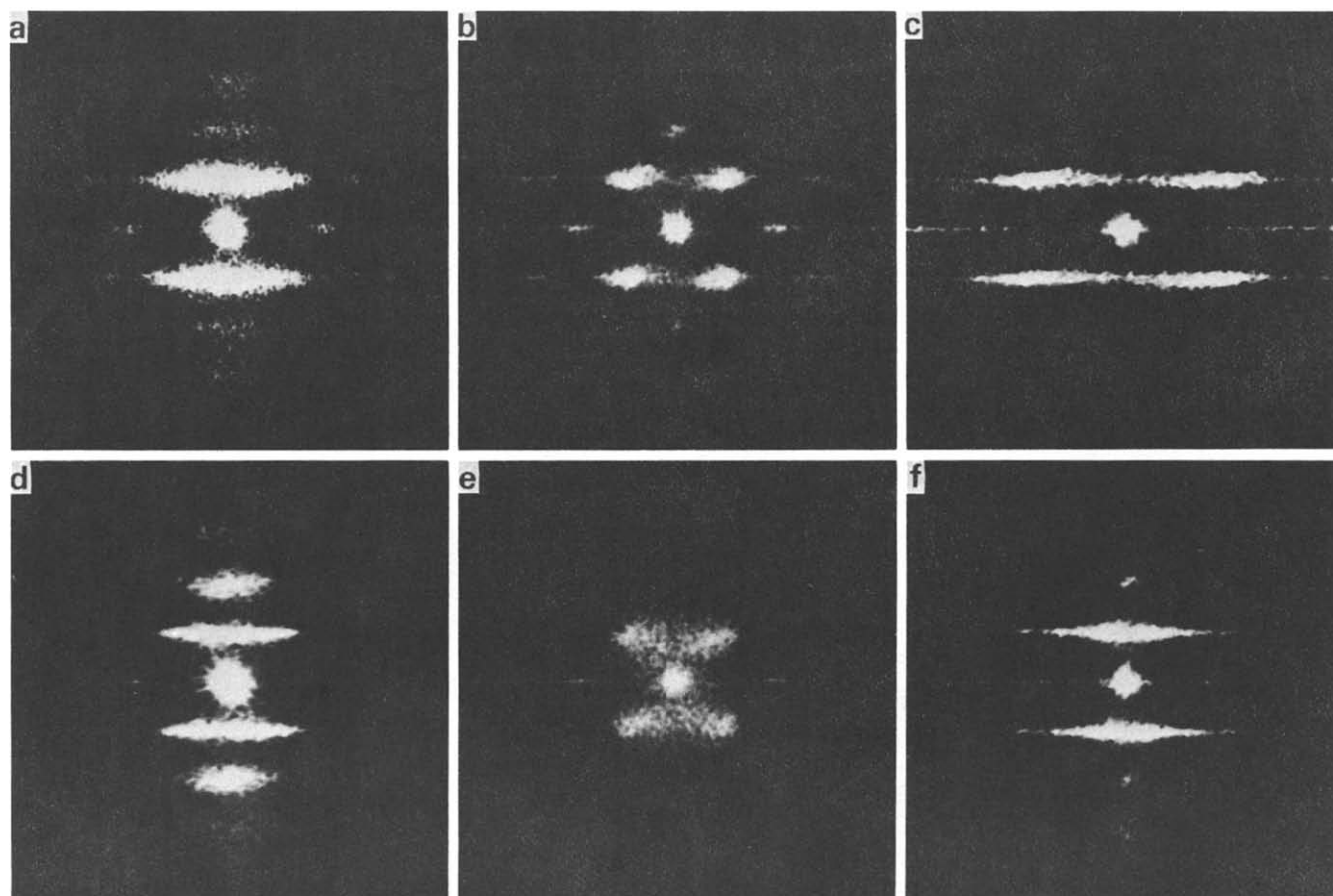In the process of drawing a complex of thermal and

Figure 6 Examples of transforms for model 3. Parameters are given in *Table 2*

Table 2 Parameters used for the masks from which the transforms of *Figure 6* were prepared

Transform	W	σ (W)	X	σ (X)	A	σ (A)	Correlation
(a)	30	5	30	5	30	5	x
(b)	30	5	30	5	30	5	√
(c)	15	5	30	5	30	5	√
(d)	30	5	50	5	10	5	√
(e)	30	5	30	20	30	5	√
(f)	30	20	30	5	30	5	√

mechanical effects occurs. The mechanical drawing orients the molecules and has a tendency to pull them out of crystalline order. On the other hand thermal activation aids crystallization. In the necking region, shearing of crystallites is a probable mechanism by which a shape function, with the asymmetry required to explain four-pointed SAXS patterns, can be produced. It is also likely that a lateral locking or correlation of crystallites occurs in much the same fashion as envisaged by Statton[17], for knobbly micro-fibrils, to give the partial, two-dimensional order that may just as easily produce the four-point pattern. It is probable that both shape and lattice effects contribute to the transition. It seems unlikely, however, that pronounced fibrillar entities are present in view of the complex tangle of molecules that

exists in the melt and of the close lateral packing needed to eliminate equatorial SAXS.

Thus, bearing in mind all the evidence available, it is envisaged that the structure for drawn polyester fibres approximates to that depicted in *Figure 7*. The crystalline regions are far from perfect and have dimensions, both along the fibre axis and laterally, approximately half that of the long period. At the boundaries of the crystallites the molecular chains will form partially-ordered, perhaps paracrystalline, material together with irregularly-folded or kinked chains. It is probable that the most extended surface of the crystallites will be parallel to the (100) planes with the result that, on drawing the yarn, this plane orients perferentially, as shown by the double orientation phenomenon that has been found in some WAXS patterns[3].
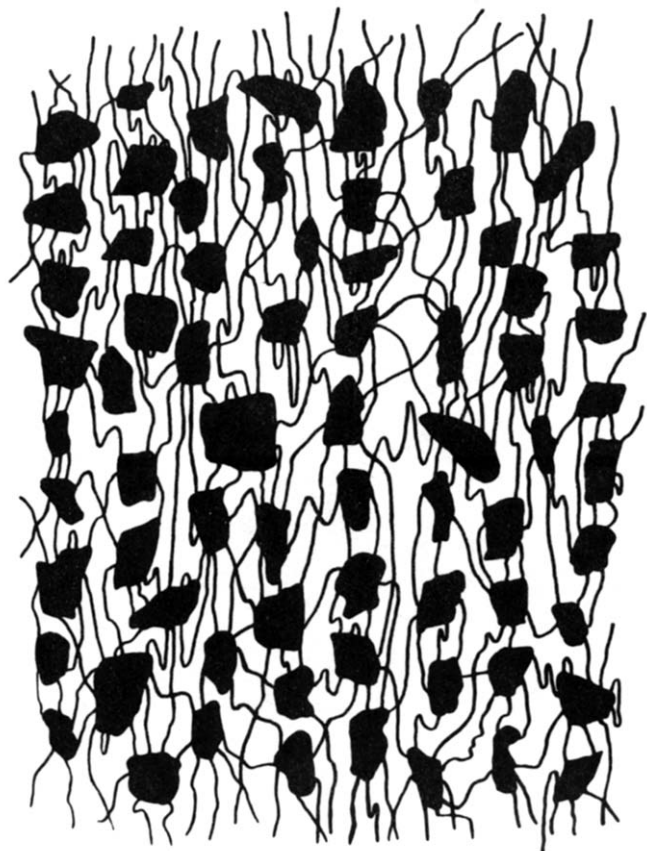
Figure 7 Proposed structure for PET fibres

REFERENCES

1 Statton, W. O. in 'Newer Methods of Polymer Characterisation' (Ed. B. Ke), Wiley Interscience, 1964, Ch. 6
2 Warwicker, J. O. *J. Appl. Polym. Sci.* 1978, **22**, 187
3 Liska, E. Chemiefasern/Textil-Industrie. 1973. Sept., 818; Oct., 964; Nov., 1109
4 Taylor, C. A. in 'Optical Transforms' (Ed. H. Lipson), Academic Press, 1972, Ch. 4
5 Mukhopadhyay, U. and Taylor, C. A. *J. Appl. Crystallogr.* 1971, **4**, 20
6 Lewis, J. W. *Ph.D. Thesis*, University of Wales, 1982
7 Warwicker, J. O. *J. Polym. Sci. A-2* 1966, **4**, 571
8 Harburn, G., Miller, J. S. and Welberry, T. R. *J. Appl. Crystallogr.* 1974, 7, 36
9 Harburn, G. and Ranniko, J. K. *J. Phys. E.* 1972, **5**, 757
10 Daubeny, R. de P., Bunn, C. W. and Brown, C. J. *Proc. Roy. Soc.* 1954, **A226**, 531
11 Arnott, S. and Wonacott, A. J. *Polymer* 1966, 7, 157
12 Guinier, A. 'X-ray Diffraction', Freeman and Co., 1963, p. 121
13 Casey, M. *Polymer* 1977, **18**, 1219
14 Warwicker, J. O. *J. Appl. Polym. Sci.* 1975, **19**, 1147
15 Miller, J. S. *Ph.D. Thesis*, University of Wales, 1975
16 Kukesenko, V. S., Orlova, O. D. and Slutsker, L. I. *Polym. Sci. USSR* 1973, **15**, 2849
17 Statton, W. O. *J. Polym. Sci.* 1959, **19**, 143